

Growth and characterization of lead bromide: application to mercurous bromide

Geug-Tae Kim[†]

Department of Chemical & Polymer Engineering, Hannam University, Taejon 306-791, Korea

(Received March 31, 2004)

(Accepted April, 2004)

Abstract Mercurous Bromide (Hg_2Br_2) crystals hold promise for many acousto-optic and opto-electronic applications. This material is prepared in closed ampoules by the physical vapor transport (PVT) growth method. We investigate the effects of solutal convection on the crystal growth rate in a horizontal configuration for diffusive-convection conditions and purely diffusion conditions achievable in a low gravity environment. Our results show that the growth rate is decreased by a factor of one-fourth with a ten reduction of gravitational acceleration near $y = 2.0 \text{ cm}$. For $0.1 g_0$, the growth rate pattern exhibits relatively flat which is intimately related to diffusion-dominated processes. The growth rate nonuniformity is regardless of aspect ratio across the interfacial positions from 0 to 1.5. Also, the effect of a factor of the ten reduction in the gravitational acceleration is same to both $\text{Ar} = 5$ and 2. The enlargement in the molecular weight of B from 50 to 500 by a factor 4 causes a decrease in the maximum growth rate by the same factor, indicative of the effect of solutal gradients.

Key words lead bromide, mercurous bromide

1. Introduction

Interest in growing Hg_2Br_2 single crystal stems from their exceptional optical properties and very broad transmission range from 0.30 to 30 μm for applications in acousto-optic and opto-electronic devices such as Bragg cells, X-ray detectors operating at ambient temperature [1]. The solid-liquid equilibrium data on the mercuric bromide (HgBr_2) and mercury (Hg) system has not been studied extensively. The available phase diagram [2] suggests that equimolar compound Hg_2Br_2 decomposes to two liquids at a temperature near 450°C where the vapor pressure is well above 20 atm. Because of this decomposition and high vapor pressure, mercurous bromide cannot be solidified as a single crystal directly from the stoichiometric melt. However, very similar to the mercurous chloride, mercurous bromide exhibits sufficiently high vapor pressure at low temperatures so that these crystals are usually grown by the physical vapor transport (PVT) in closed silica glass ampoules. The PVT processing has many advantages over melt-growth methods since it can be conducted at low temperatures: (1) vapor-solid interfaces possess relatively high interfacial morphological stability against non-uniformities in heat and mass transfer; (2) high purity crystals are achieved;

(3) materials decomposed before melting, such as Hg_2Br_2 can be grown; (4) lower point defect and dislocation densities are achieved [3]. The mechanism of the PVT process is simple: sublimation-condensation in closed silica glass ampoules in temperature gradient imposed between the source material and the growing crystal. In the PVT system of Hg_2Br_2 , the molecular species Hg_2Br_2 sublimates as the vapor phase from the crystalline source material (Hg_2Br_2), and is subsequently transported and re-incorporated into the single crystalline phase (Hg_2Br_2) [4]. Recently PVT has become an important crystal growth process for a variety of acousto-optic materials. However, the industrial applications of the PVT process remain limited. An important main reason is that transport phenomena occurring in the vapor are complex and coupled so that it is difficult to design or control the process accurately. Such complexity and coupling are associated with the inevitable occurrence of thermal convection generated by the interaction of gravity with density gradients arising from temperature gradients. Thermal convection has been regarded as detrimental and, thus, to be avoided or minimized in PVT growth system. These thermal convection-induced complications result in problems ranging from crystal inhomogeneity to structural imperfection. Therefore, in order to analyze and control the PVT process accurately, and also make significant improvements in the process, it is essential to investigate the roles of thermal convection in the PVT process.

[†]Corresponding author
Tel: +82-42-629-7984
Fax: +82-42-623-9489
E-mail: gtkim@mail.hannam.ac.kr

The literature on pure thermal convection without crystal growth in enclosures, is much more extensive than that of thermal convection associated with vapor-crystal growth in enclosures, i.e., with mass fluxes across and at the solid-fluid interfaces (called interfacial fluxes). Recently some models have been presented to describe the flow patterns and to study the effects of thermal convection in enclosures for vapor-crystal growth. The first treatment of an analytical solution of the two-dimensional chemical vapor transport was published by Klosse and Ullersma (KU) [5], and extended by Jhaveri and Rosenberger [6] who compared with KU's model and revealed that up to moderately large Grashof numbers, KU's model gives a reasonably good estimate of the convective transport system in two dimensions. They also showed that convection causes a strong nonuniformity in the interfacial growth flux. Thermosolutal convection in PVT process with conduction at crystal and source regions inside a horizontal rectangular enclosure has been modeled [7]. Weaver and Viskanta [8] published calculations on thermosolutal convection with variable properties in binary gases for rectangular enclosures similar to vapor-crystal system, i.e., with sublimation-condensation boundary conditions. Extrémet *et al.* [9] examined thermal and/or solutal convection for a two-dimensional horizontal rectangular system with aspect ratios (height-to-transport length) ranging between 0.1 and 0.5 in a three zone furnace. These studies, in the main, were confined to the case when the horizontal temperature gradients were prescribed in a horizontal cylinder or rectangular geometry with differentially heated end walls. With regard to vertical enclosures, there are few studies on thermal convection either with vapor crystal growth or without. Pure thermal convection in vertical enclosure systems is similar to the classical Rayleigh-Bénard (RB) problem, in the sense that there is an adverse vertical temperature gradient, however, it differs from the classical RB flow in that there are side walls present. Olson and Rosenberger [10, 11] studied experimentally the RB flow for a monocomponent and two-component fluid without interfacial fluxes in vertical cylindrical enclosures differentially heated from below. The results showed that the convective motion in the cylinder with impermeable boundaries was entirely different from that in the RB flow. The critical Rayleigh number for onset of a single convection cell was 220 (based on R^4/L in the critical Rayleigh number instead of L^3 in which R and L are the radius and height of the cylinder respectively), being about 5% lower than theory. Asymmetric flow patterns were observed to occur at high Rayleigh

numbers.

Markham, Greenwell and Rosenberger [12] examined the effects of thermal and thermosolutal convections during the PVT process inside vertical cylindrical enclosures for a time-independent system, and showed that even in the absence of gravity, convection can be present, causing nonuniform concentration gradients. They emphasized the role of geometry in the analysis of the effects of convection. As such these fundamentally constitute steady state two-dimensional models. The steady state models are limited to low Rayleigh number applications, because as the Rayleigh number increases oscillation of the flow field occurs. To address the issue of unsteady flows in PVT, Duval [13] performed a numerical study on transient thermal convection in the PVT processing of Hg_2Cl_2 very similar to the mercurous bromide for a vertical rectangular enclosure with insulated temperature boundary conditions for Rayleigh numbers up to 10^6 . Duval [14] has also shown the bifurcation sequences which lead to chaotic flow in PVT processing. Nadarajah *et al.* [15] addressed the effects of solutal convection for any significant disparity in the molecular weights of the crystal components and the inert gas. Zhou *et al.* [16] reported that the traditional approach of calculating the mass flux assuming one-dimensional flow for low vapor pressure systems is indeed correct. Rosenberger *et al.* [17] studied three-dimensional numerical modeling of the PVT yielded quantitative agreement with measured transport rates of iodine through octofluorocyclobutane (C_4F_8) as inert background gas in horizontal cylindrical ampoules.

In this numerical study, a two-dimensional model is used for the analysis of the PVT processes during vapor-growth of mercurous bromide crystals (Hg_2Br_2) in vertically oriented, cylindrical, closed ampoules in a two-zone furnace system. Mass transfer-limited processes are considered in this paper, although the recent paper of Singh, Mazelsky and Glicksman [18] demonstrated that the interface kinetics plays an important role in the PVT system of Hg_2Cl_2 very similar to the mercurous bromide. Only thermal convection will be considered at this point, primarily because the Hg_2Br_2 source materials are highly purified in the actual crystal growth process, and consequently solutally-induced convection can be ignored in comparison to thermal convection. All results presented in this paper are for a mixture of Hg_2Br_2 vapor containing some impurity such as carbon monoxide.

It is the purpose of this paper (1) to discuss the development of a mathematical model for single crystals inside a PVT reactor, incorporating the mass transfer-limited

model with idealized boundary conditions, (2) to relate the applied convective process parameters to crystal growth rate and its interfacial distributions, (3) to examine the effects of solutal convection with a linear temperature profile in order to gain insights into the underlying physicochemical processes.

2. The Model

Consider a rectangular enclosure of height H and transport length L , shown in Fig. 1. The source is maintained at a temperature T_s , while the growing crystal is at a temperature T_c , with $T_s > T_c$. PVT of the transported component A occurs inevitably, due to presence of impurities, with the presence of an inert component B (CO). The interfaces are assumed to be flat for simplicity. The finite normal velocities at the interfaces can be expressed by Stefan flow deduced from the one-dimensional diffusion-limited model [19], which provide the coupling between the fluid dynamics and species calculations. On the other hand, the tangential component of the mass average velocity of the vapor at the interfaces vanishes. Thermodynamic equilibria are assumed at the interfaces so that the mass fractions at the interfaces are kept constant at $\omega_{A,s}$ and $\omega_{A,c}$. On the vertical non-reacting walls an appropriate velocity boundary condition is no-slip, the normal concentration gradient is zero, and temperature is imposed as a linear temperature gradient and an asymmetric horizontal temperature gradient. The asymmetry is attributable to temperature differences between two opposite walls.

Thermophysical properties of the fluid are assumed to be constant, except for the density. When the Boussinesq approximation is invoked, density is assumed constant except the buoyancy body force term. The density is assumed to be a function of temperature and not of

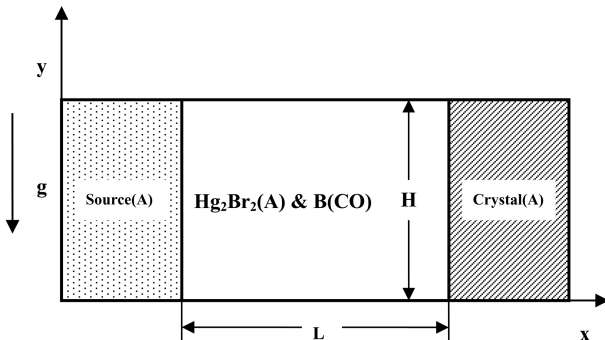


Fig. 1. Schematic of PVT growth reactor in a two-dimensional rectangular system.

concentration. The ideal gas law and Dalton's law of partial pressures are used. Viscous energy dissipation and the Soret-Dufour (thermo-diffusion) effects can be neglected, as their contributions remain relatively insignificant for the conditions encountered in our PVT crystal growth processes. Radiative heat transfer can be neglected under our conditions, based on Kassemi and Duval [20].

The transport of fluid within a rectangular PVT crystal growth reactor is governed by a system of elliptic, coupled conservation equations for mass (continuity), momentum, energy and species (diffusion) with their appropriate boundary conditions. Let v_x , v_y denote the velocity components along the x - and y -coordinates in the x , y rectangular coordinate, and let T , ω_A , p denote the temperature, mass fraction of species A (Hg_2Br_2) and pressure, respectively.

The dimensionless variables are scaled as follows:

$$x^* = \frac{x}{H}, \quad y^* = \frac{y}{H}, \quad (1)$$

$$u = \frac{u_x}{U_c}, \quad v = \frac{v_y}{U_c}, \quad p = \frac{p}{\rho_c U_c^2}, \quad (2)$$

$$T^* = \frac{T - T_c}{T_s - T_c}, \quad \omega_A^* = \frac{\omega_A - \omega_{A,c}}{\omega_{A,s} - \omega_{A,c}}. \quad (3)$$

$$\nabla^* \cdot \nabla^* = 0, \quad (4)$$

$$\vec{\nabla}^* \cdot \nabla^* \vec{\nabla}^* = -\nabla^* p^* + \text{Pr} \nabla^{*2} \vec{\nabla}^* - \text{Ra} \cdot \text{Pr} \cdot T^* \cdot \mathbf{e}_g, \quad (5)$$

$$\vec{\nabla}^* \cdot \nabla^* T^* = \nabla^{*2} T^* \quad (6)$$

$$\vec{\nabla}^* \cdot \nabla^* \omega_A^* = \frac{1}{\text{Le}} \nabla^{*2} \omega_A^* \quad (7)$$

The dimensionless governing equations are given by:

These nonlinear, coupled sets of equations are numerically integrated with the following boundary conditions:

On the walls ($0 < x^* < L/H$, $y^* = 0$ and 1):

$$u(x^*, 0) = u(x^*, 1) = v(x^*, 0) = v(x^*, 1) = 0 \quad (8)$$

$$\frac{\partial \omega_A^*(x^*, 0)}{\partial y^*} = \frac{\partial \omega_A^*(x^*, 1)}{\partial y^*} = 0,$$

$$T^*(x^*, 0) = T^*(x^*, 1) = \frac{1}{-\text{Ar}} \cdot x^* + 1$$

On the source ($x^* = 0$, $0 < y^* < 1$):

$$u(0, y^*) = -\frac{1}{\text{Le}(1 - \omega_{A,s})} \frac{\Delta \omega}{\partial x^*} \frac{\partial \omega_A^*(0, y^*)}{\partial x^*}, \quad (9)$$

$$v(0, y^*) = 0,$$

$$T^*(0, y^*) = 1,$$

$$\omega_A^*(0, y^*) = 1.$$

On the crystal ($x^* = L/H$, $0 < y^* < 1$):

$$u(L/H, y^*) = \frac{1}{Le(1-\omega_{A,s})} \frac{\Delta\omega}{\partial x^*} \frac{\partial \omega_A^*(L/H, y^*)}{\partial x^*}, \quad (10)$$

$$v(L/H, y^*) = 0,$$

$$T^*(L/H, y^*) = 0,$$

$$\omega_A^*(L/H, y^*) = 0.$$

Interfacial velocities (sublimation and condensation velocities) in equations (9) and (10)

$$u(0, y^*) = \frac{Ar}{Pe(C_v-1)} \frac{\partial \omega_A^*(0, y^*)}{\partial x^*} \quad (11)$$

$$u(L/H, y^*) = \frac{Ar\Delta\omega}{Pe C_v} \frac{\partial \omega_A^*(L/H, y^*)}{\partial x^*} \quad (12)$$

can also be expressed in terms of a dimensionless Peclet number and a concentration parameter as follows:

$$Pe = \frac{U_{adv}L}{D_{AB}}, \quad C_v = \frac{1-\omega_{A,c}}{\Delta\omega}. \quad (13)$$

The Peclet number can be also estimated by thermodynamic variables:

$$Pe = \ln\left(\frac{p_B(L)}{p_B(0)}\right). \quad (14)$$

U_{adv} is a characteristic velocity which depends on the thermodynamics of PVT processes, i.e., the vapor pressure of Hg_2Br_2 as a function of temperature. The mass fraction at the solid-vapor interfaces is fixed at the corresponding temperature. Thus for a given set of conditions, the mass fraction can not be varied independently.

Since the total vapor pressure can be taken to be constant during the physical vapor transport, the mass fraction of species A is defined as

$$\omega_A = \frac{\rho_A}{\rho},$$

$$\rho = \frac{p_A M_A}{R_g T}; \quad \rho_B = \frac{p_B M_B}{R_g T}.$$

where $\rho = \rho_A + \rho_B$. From the ideal gas law, the density of species A(B) is related to the partial pressure as

$$\omega_A = \frac{p_A M_A}{p_A M_A + (P_T - p_A) M_B}, \quad (15)$$

Thus,

which can be rearranged to give

$$\omega_A = \frac{1}{1 + (P_T/p_A - 1)M_B/M_A}. \quad (16)$$

The vapor pressure [21] p_A of Hg_2Br_2 (in the unit of

Pascal) can be evaluated from the following formula as a function of temperature:

$$p_A = e^{(a-b/T)}, \quad (17)$$

in which $a = 29.75$, $b = 11767.1$. P_T denotes the total pressure, and the partial pressures for A(B) are denoted by $p_A(p_B)$.

The crystal growth rate v_c is calculated from a mass balance at the crystal vapor interface, assuming fast kinetics, i.e. all the vapor is incorporated into the crystal, which is given by (subscripts c, v refer to crystal and vapor respectively)

$$\int \rho_v v_v \cdot n dA = \int \rho_c v_c \cdot n dA, \quad (18)$$

$$v_c = \frac{\rho_v \int v_v \cdot n dA}{\rho_c \int dA}. \quad (19)$$

3. Results and Discussion

The parametric study is useful for showing trends and generalizing the problem, but many parameters are involved in the problem under consideration, which renders it difficult for a general analysis. One of the purposes for this study is to correlate the growth rate and the interfacial distributions to process parameters for a particular material (Hg_2Br_2). Thus, it is desirable to express some results in terms of dimensional growth rate, however they are also applicable to parameter ranges over which the process varies in the manner given. The six dimensionless parameters, namely Gr, Ar, Pr, Le, C_v and Pe, are independent and arise naturally from the dimensionless governing equations and boundary conditions. The physical properties and operating conditions used in this study are listed in Table 1.

In this study, the effects of the solutal convection and gravitational acceleration perturbations on the crystal growth and its distributions across an interface. When solutal convection dominates, the imposed temperature profile has little effect on the growth rate [15].

Conductive wall boundary conditions with a linear temperature profile are considered, while the insulated walls are not considered because it is difficult to obtain in practice and most of vapor growth experiments are performed under the imposed temperature profiles to avoid nucleation at the ampoule walls.

Figure 2 shows the effects of gravitational accelerations on the crystal growth rate for the interfacial distributions in a horizontal system of aspect ratio 5 ($L = 10$

Table 1
Typical thermo-physical properties used in simulations ($M_A = 560.988$, $M_B = 28$)

Transport length, L	10 cm
Height, H	2 cm
Source temperature, T_s	320°C
Crystal temperature, T_c	300°C
Density, ρ	0.00204 g/cm ³
Dynamic viscosity, μ	0.14 g/cm-sec
Diffusivity, D_{AB}	0.87 cm ² /s
Thermal expansion coefficient, β	0.0017 K ⁻¹
Prandtl number, Pr	0.74
Lewis number, Le	0.28
Peclet, Pe	2.82
Concentration number, C_v	1.06
Total system pressure, P_T	193 Torr
Thermal Grashof number, Gr_t	1.34×10^4
Solutal Grashof number, Gr_s	2.18×10^5

cm, $H = 2$ cm), with a source temperature $T_s = 320^\circ\text{C}$, a crystal temperature $T_c = 300^\circ\text{C}$, an impurity (CO) pressure of 10 Torr and an acceleration of $1g_0$ in the positive y -direction, where g_0 denotes the standard gravitational acceleration constant, 980.665 cm/s^2 . For $g_y = 1g_0$, the corresponding dimensionless parameters are thermal Grashof number $Gr_t = 1.34 \times 10^4$, solutal Grashof number $Gr_s = 1.34 \times 10^4$, $Ar = 5$, $Pr = 0.74$, $Le = 0.28$, $C_v = 1.06$ and $Pe = 2.82$ with the total pressure of 193 Torr. The convection causes significant nonuniformities in the growth rate across the interface in the crystal region, which is consistent with the results of Markham *et al.*

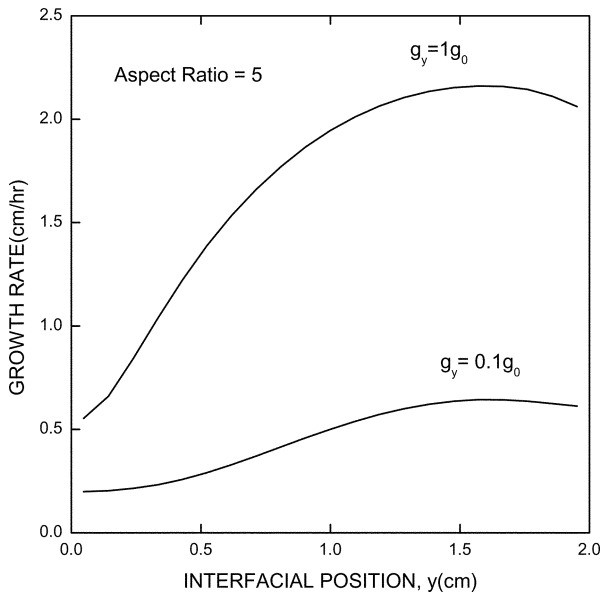


Fig. 2. Interfacial distribution of crystal growth rate of Hg_2Br_2 for a horizontal ampoule of aspect ratio of 5, with a linear temperature profile between $T_s = 320$ and $T_c = 300^\circ\text{C}$, and $g_y = 1g_0$, and $0.1g_0$.

[12]. As not shown here, the parabolic patterns of growth rate distributions indicate one single convection roll occurs toward the growing interface. The growth rate is decreased by a factor of one-fourth with a ten reduction of gravitational acceleration near $y = 2.0$ cm. For $0.1 g_0$, the growth rate pattern exhibits relatively flat which is intimately related to diffusion-dominated processes. In other words, diffusive transport dominates convective flows under the microgravity environments. Also, the growth rate is more sensitive to the perturbation of gravitational acceleration for the regions from 0 through 1.0 than those from 1.0 through 2.0 cm. This is due to the occurrence of convective roll, which provides vapor supersaturated in component A in front of the growing crystal regions. When thermal convection is dominated an oppositely rotating roll would appear because of thermally buoyancy-driven effects, i.e., chimney effects and, thus, in enhanced growth in the upper half of the growing crystal interface. Figure 3 shows the results for a system with same parameters as in Fig. 2 for an aspect ratio of 2 ($L = 4$ cm). For a $1 g_0$ level, the maximum growth rate is larger than for aspect ratio of 5 by a factor of 1.7. For regions from 0 to 1.5, the growth nonuniformities due to convection are increased by a factor of 4 in both $Ar = 5$ and 2. The growth rate nonuniformity is regardless of aspect ratio across the interfacial positions from 0 to 1.5. Also, the effect of a factor of the ten reduction in the gravitational acceleration is

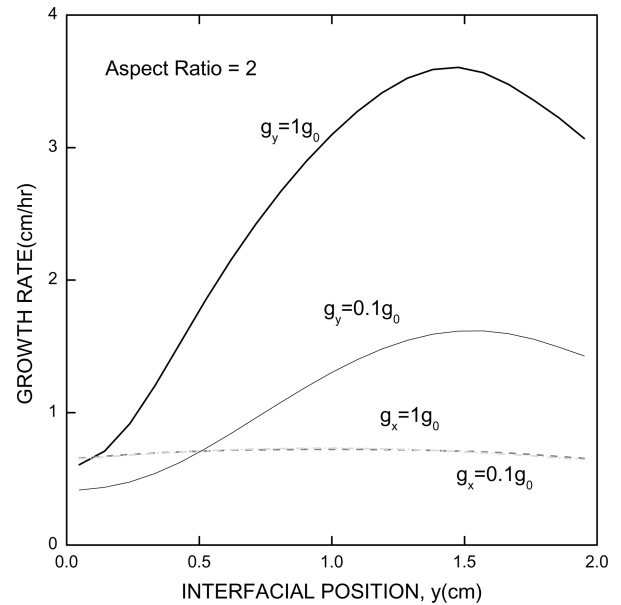


Fig. 3. Interfacial distribution of crystal growth rate of Hg_2Br_2 for an ampoule of aspect ratio of 2, with a linear temperature profiles between $T_s = 320^\circ\text{C}$ and $T_c = 300^\circ\text{C}$, and $g_y = 1g_0$, $0.1g_0$, and $g_x = 1g_0$, $0.1g_0$.

same to both $Ar = 5$ and 2 , indicating that variations in aspect ratio have an influence on increasing the convective intensity, but on not changing the essence of convection such as flow structures under considerations. The ten reduction in the gravitational level is enough to suppress convective effects on the growth rate for $Ar = 5$ (Fig. 2) and 2 (Fig. 3). In the vertical position convection with a bottom-source, the variations in the gravitational levels were found to be insignificant for the growth nonuniformities. This is likely to be due to “bottom-heavy” density stratification [15], which means the growth ampoule is positioned in the convectively stabilizing orientation. Note that in the horizontal orientation to the gravity direction, density gradients always give rise to convection. As shown in Fig. 3, the variations of nonuniformities due to convection are likely to be more significant in the horizontal orientation of the ampoule than in the vertical position.

Figure 4. shows the results of the effects of the position of the ampoule on the growth rate. For $Ar = 2$, the growth rates for the top-source are much larger than the bottom-source. A factor of ten reduction in the gravitation is more significant in the horizontal orientation than in the top-source: for the maximum growth rate, a factor of 2.5 is for the horizontal, on the other hand, a factor of 1.5 is for the top-source. Figure 5 shows that increasing the temperature difference between source and crystal for $Ar = 5$, from 20 K to 30 K, under otherwise unchanged conditions, gave similar results to Fig.

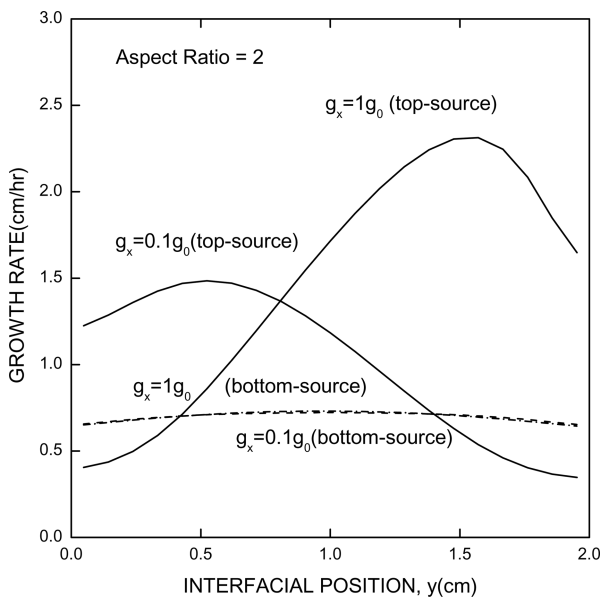


Fig. 4. Interfacial distribution of crystal growth rate of Hg_2Br_2 for the same system as in Fig. 3, with g_y (top-source) = $1g_0$, $0.1g_0$, and g_x (bottom-source) = $1g_0$, $0.1g_0$.

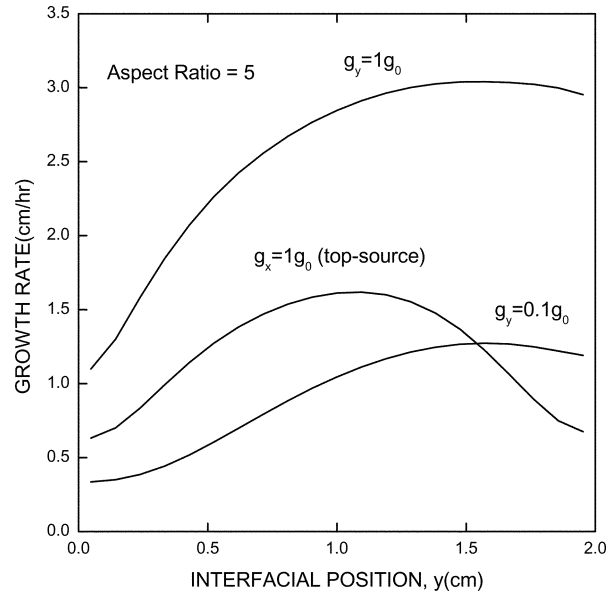


Fig. 5. Interfacial distribution of crystal growth rate of Hg_2Br_2 for an ampoule of aspect ratio of 2, with a linear temperature profile between $T_s = 330^\circ C$ and $T_c = 300^\circ C$, and $g_y = 1g_0$, $0.1g_0$, and g_x (top-source) = $1g_0$.

2. For the horizontal orientation with $1g_0$, as the temperature difference increases by 10 K, it can be seen that the maximum growth rate is increased by 1.0 cm/hr. One sees that when the same system was positioned vertically with source up (top-source), for an axial acceleration of $1g_0$, a reduction in growth rate to one half and the maximum growth rate are obtained near the center of the interfacial positions, $y = 1$ cm. From a viewpoint of the maximum growth rate, there is little significant difference between the systems with a space environment of $0.1g_0$ and with top-source positioned orientation.

Figure 6 shows the effects of molecular weight M_B on interfacial distribution of crystal growth rates for a horizontal ampoule of $Ar = 5$, with linear wall temperature profiles between $T_s = 320^\circ C$ and $T_c = 300^\circ C$, and $g_y = 1g_0$. As the molecular weight of B is increased from 2 to 28, the effect of solutal convection increases, which reflects an increase in the growth rate, and then, as the weight decreases to 50, it decreases slowly, and then decreases rapidly with increasing the weight up to 200, and eventually the convection mode is switched over diffusion-dominant mode. It is known that when the molecular weights of A are closer to that of impurity material, B, thermal convection would be dominant over solutal convection [15]. Therefore, the nonuniformities of growth rate for $M_B = 500$ and 560.988 (CO) suggests the oppositely rotating roll (clockwise) to the convective roll based on solutal convection (counter-clock-

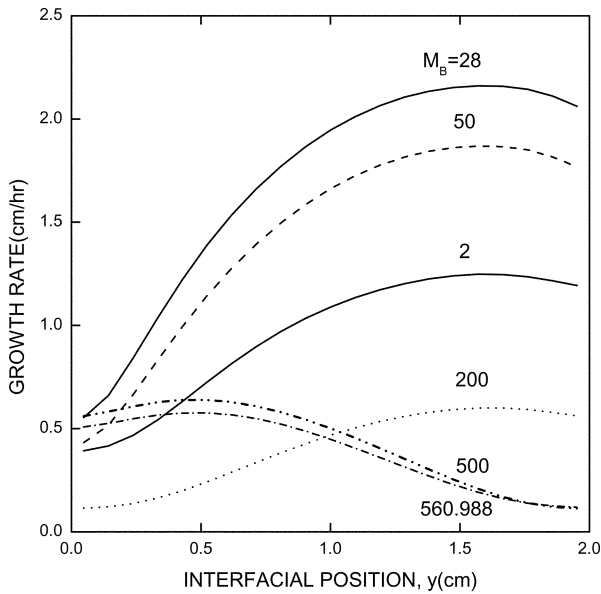


Fig. 6. The effects of molecular weight M_B on interfacial distribution of crystal growth rates for a horizontal ampoule of $Ar = 5$, with a linear wall temperature profile between $T_s = 320^\circ\text{C}$ and $T_c = 300^\circ\text{C}$, and $g_y = 1g_0$.

wise). The enlargement in the molecular weight of B from 50 to 500 by a factor 4 causes a decrease in the maximum growth rate by the same factor, indicative of the effect of solutal gradients.

Figure 7 shows the axial distribution of partial pressure of component A at the walls resulting from purely diffusive transport for a system with $Ar = 5$, $T_s = 320^\circ\text{C}$ and $T_c = 300^\circ\text{C}$, and $g_y = 1g_0$, and $M_B = 28$. The equi-

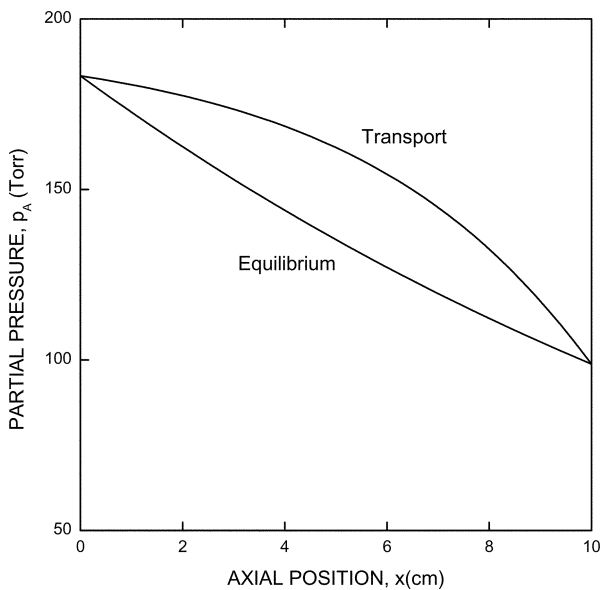


Fig. 7. The axial distribution of partial pressure of component A at the walls resulting from purely diffusive transport for a system with $Ar = 5$, $T_s = 320^\circ\text{C}$ and $T_c = 300^\circ\text{C}$, and $g_y = 1g_0$, and $M_B = 28$.

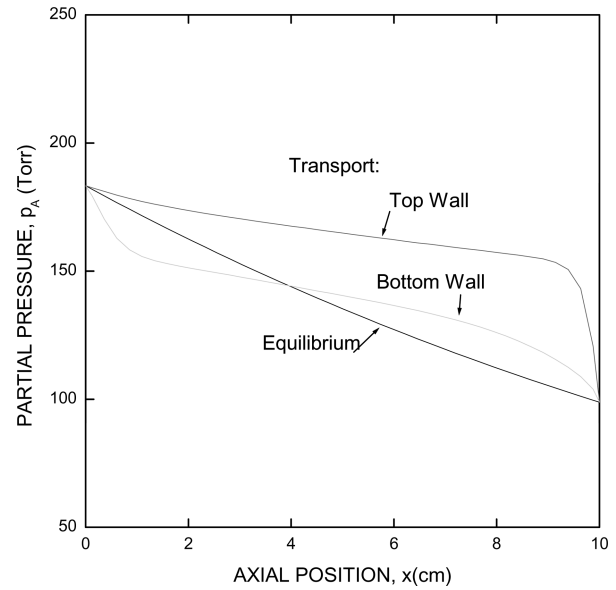


Fig. 8. The axial distribution of partial pressures of component A at the top and bottom walls due to diffusive-convective transport in the system same as in Fig. 7.

librium vapor pressure of component A is calculated from Eq. (17), while the partial pressure of A at the walls of the ampoule is computed based on purely diffusive transport. It should be noted that it is observed a purely diffusive solution only $10^{-4} g_0$ [22]. Figure 8 shows axial distribution of partial pressures of component A at the top and bottom walls due to diffusive-convective transport in the same system as in Fig. 7. The supersaturation of vapor A along the top walls is held which might yield undesirable nucleations at the top walls, i.e., parasitic nucleation at the walls. The partial pressure at the top wall is larger than the bottom wall so that the solutal convective flow structure is likely to be counter-clockwise.

4. Conclusions

In the past years considerable progress has been achieved in modeling PVT processes. Our study covers the effects of solutal convection on the growth rate of Hg_2Br_2 crystals and interfacial distributions in a rectangular ampoule under terrestrial and micro-gravitational conditions for various operating parameters. Taking into account the real thermodynamical dependency of the mass fraction as a function of temperature reduces considerably the control we have on the process. The growth rate and convective magnitude of PVT were studied by isolating the trends of solutal convection from the combination of thermosolutal convection. We

studied solutal convection at low thermally driven density gradients. Our results show the growth rate nonuniformity is regardless of aspect ratio across the interfacial positions from 0 to 1.5. Also, the effect of a factor of the ten reduction in the gravitational acceleration is same to both $Ar = 5$ and 2. In the vertical position convection with a bottom-source, the variations in the gravitational levels were found to be insignificant for the growth nonuniformities. This is likely to be due to "bottom-heavy" density stratification, which means the growth ampoule is positioned in the convectively stabilizing orientation. The enlargement in the molecular weight of B from 50 to 500 by a factor 4 causes a decrease in the maximum growth rate by the same factor, indicative of the effect of solutal gradients.

Acknowledgement

This work was financially supported by Korea Sanhak Foundation Grant (2002~2003).

References

- [1] N.B. Singh, M. Gottlieb, G. B. Brandt, A.M. Stewart, R. Mazelsky and M. E. Glicksman, "Growth and characterization of mercurous halide crystals:mercurous bromide system", *J. Crystal Growth* 137 (1994) 155.
- [2] Dworsky and K.Komarek, *Monatsh. Chem.* 101 (1970) 976.
- [3] F. Rosenberger, "Fluid dynamics in crystal growth from vapors", *Physico-Chemical Hydro-dynamics* 1 (1980) 3.
- [4] N.B. Singh, M. Gottlieb, A.P. Goutzoulis, R.H. Hopkins and R. Mazelsky, "Mercurous Bromide acousto-optic devices", *J. Crystal Growth* 89 (1988) 527.
- [5] K. Klosse and P. Ullersma, "Convection in a chemical vapor transport process", *J. Crystal Growth* 18 (1973) 167.
- [6] B.S. Jhaveri and F. Rosenberger, "Expansive convection in vapor transport across horizontal rectangular enclosures", *J. Crystal Growth* 57 (1982) 54.
- [7] Christopher Mennetrier and Walter M.B. Duval, "Thermal-solutal convection with conduction effects inside a rectangular enclosure", NASA TM 105371, December (1991).
- [8] J.A. Weaver and R. Viskanta, "Natural convection due to horizontal temperature and concentration gradients - I. Variable thermophysical property effects", *J. Heat Mass Transfer* 34 (1991) 3107.
- [9] G.P. Extrémet, B. Roux, P. Bontoux and F. Elie, "Two-dimensional model for thermal and solutal convection in multizone physical vapor transport", *J. Crystal Growth* 82 (1987) 761.
- [10] J.M. Olson and F. Rosenberger, "Convective instabilities in a closed vertical cylinder heated from below. Part 1. Monocomponent gases", *J. Fluid Mech.* 92 (1979) 609.
- [11] J.M. Olson and F. Rosenberger, "Convective instabilities in a closed vertical cylinder heated from below. Part 2. Binary gas mixtures", *J. Fluid Mech* 92 (1979) 631.
- [12] B.L. Markham, D.W. Greenwell and F. Rosenberger, "Numerical modeling of diffusive-convective physical vapor transport in cylindrical vertical ampoules", *J. Crystal Growth* 51 (1981) 426.
- [13] Walter M.B. Duval, "Convection in the physical vapor transport process-- I: Thermal", *J. Chemical Vapor Deposition* 2 (1994) 188.
- [14] Walter M.B. Duval, "Transition to chaos in the physical transport process--I", the Proceeding of the ASME--WAM Winter Annual meeting, Fluid mechanics phenomena in microgravity, ASME-WAM, New Orleans, Louisiana, Nov. 28 -- Dec. 3, AMD-174, FED-175 (1993) 51.
- [15] A. Nadarajah, F. Rosenberger and J. Alexander, "Effects of buoyancy-driven flow and thermal boundary conditions on physical vapor transport", *J. Crystal Growth* 118 (1992) 49.
- [16] H. Zhou, A. Zebib, S. Trivedi and W.M.B. Duval, "Physical vapor transport of zinc-telluride by dissociative sublimation", *J. Crystal Growth* 167 (1996) 534.
- [17] F. Rosenberger, J. Ouazzani, I. Viohl and N. Buchan, "Physical vapor transport revised", *J. Crystal Growth* 171 (1997) 270.
- [18] N.B. Singh, R. Mazelsky and M.E. Glicksman, "Evaluation of transport conditions during PVT: mercurous chloride system", *PhysicoChemical Hydrodynamics* 11 (1989) 41.
- [19] F. Rosenberger and G. Mller, "Interfacial transport in crystal growth, a parameter comparison of convective effects", *J. Crystal Growth* 65 (1983) 91.
- [20] M. Kassemi and Walter M.B. Duval, "Interaction of surface radiation with convection in crystal growth by physical vapor transport", *J. Thermophys. Heat Transfer* 4 (1989) 454.
- [21] H. Oppermann, "Chemical aspects of Hg_2X_2 -decomposition, barogram-diagram and thermodynamic data", Proceedings of the 2nd Intl symposium on univalent mercury halides, Czechoslovakia (1989).
- [22] B. Zappoli, C. Mignon, J. C. Launay and H. Debegnac, "Germanium epitaxial growth in closed ampoules II. Numerical modeling", *J. Crystal Growth* 94 (1983) 783.